Chapter 6

AXIAL-LIGAND INFLUENCE ON P450 REDUCTION POTENTIALS: IMPLICATIONS FOR CATALYSIS

Portions of this work are excerpted with permission from:

P. S. Coelho, Z. J. Wang, M. E. Ener, S. A. Baril, A. Kannan, F. H. Arnold, E. M. Brustad. *Nat. Chem. Biol*. **2013**, 485-487.

6.1. Background: Controlled electron flow through P450

Initiation of catalysis by cytochrome P450 heme enzymes requires the controlled flow of electrons. In the native catalytic cycle, the redox cofactor NAD(P)H supplies necessary reducing equivalents, which are shuttled to the P450 heme active site via the redox cofactors flavin adenine dinucleotide (FAD) and flavin mononucleotide (FMN) that are housed in cytochrome P450 reductases. The self-sufficient enzyme P450 BM3 from the soil bacterium *B. megaterium* contains a flavin reductase domain fused to the heme domain (**Figure 6.1**), which facilitates reduction of the heme[1] and allows for high turnover rates (> 10^3 per minute).[2]

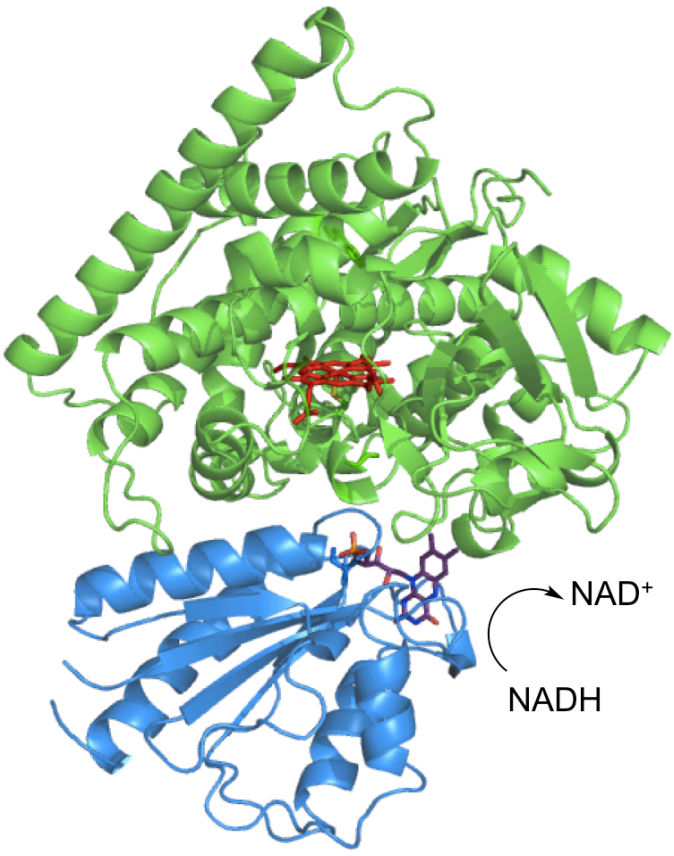

Figure 6.1. Structure of P450 BM3. (PDB: 1BVY) The oxygenase domain is colored green (heme: red), and the reductase domain is colored blue (flavin: purple). All images of protein structures in this Chapter were made using PyMol graphics software for Mac.

In many P450s, including P450 BM3, an important gating mechanism controls this electron flow by modulating the heme reduction potential in the presence or absence of substrate. As described in Chapter 1, the resting state enzyme is low-spin, six-coordinate ferric, where the distal ligation site is occupied by a water molecule; the reduction potential of this species is too negative to be efficiently reduced by NADH via the flavin cofactors. The binding of native substrates displaces the labile water molecule, inducing a positive shift in reduction potential that allows heme reduction.

Controlled electron flow is a critical element of all P450 redox chemistry, including engineered catalytic reactivity. We became interested in electron flow in a series of P450 BM3 mutants designed by Frances Arnold's group at Caltech that catalyze the cyclopropanation of styrene by ethyldiazoacetate (EDA) (**Figure 6.2**). Directed evolution was used to generate P450 mutants that display high levels of regioselectivity (for either *cis* or *trans* isomers) and enantioselectivity in such cyclopropanation reactions.[3] In analogy to the native P450 cycle (**Figure 6.3**, left), and by comparison to the mechanisms for small molecule metalloporphyrin-catalyzed cyclopropanations, the Arnold group proposed a catalytic scheme for the reactivity of engineered P450s (**Figure 6.3**, right).

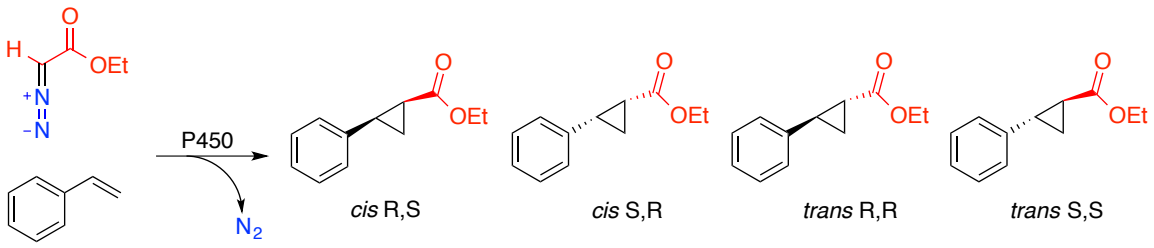

Figure 6.2. P450-catalyzed cyclopropanation of styrene.

Just as in the native catalytic cycle, reduction of the ferric resting state is essential to initiate P450-catalyzed cyclopropanation activity. This is supported

experimentally supported by the inactivity of *ferric* enzyme in the presence of EDA and styrene, and by the requirement of reductant to initiate catalysis. Furthermore, the net reaction is inhibited by carbon monoxide, which readily binds to ferrous hemes, but not ferric.[4]

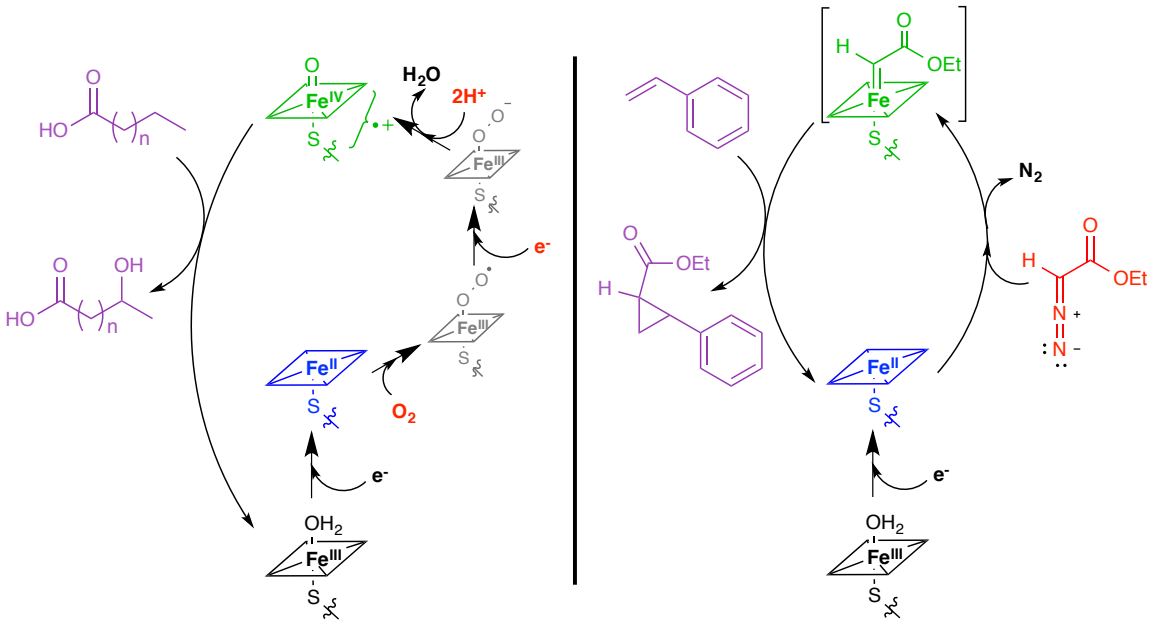

Figure 6.3. Schemes for native and engineered P450 catalysis. **Left**: Consensus P450 catalytic cycle for oxygenations, showing hydroxylation of a fatty acid. **Right**: Proposed catalytic scheme for the cyclopropanation of styrene.

Strong reductants, such as dithionite, are required to initiate catalysis in these mutants; very low levels of activity were observed in the presence of the biological reductant NADH. It was presumed that styrene was ineffective at displacing the labile water molecule and opening the electron gate; a low binding affinity is indicated by the Michaelis-Menten constant (K_M ~ 5 mM).[3] This can be circumvented for solutions of purified enzyme; dithionite can easily be added to solutions. However, the development of enzymatic cyclopropanation for sustainable, industrial scale production would be greatly enhanced by extension to

whole cell biocatalyst systems. In that case, the reductant scope is limited to endogenously produced redox cofactors, including NADH.

Enzyme engineering to more tightly bind styrene could facilitate the substrate gating issue, but this process would need to be repeated for each new substrate, and the P450 catalyst would lose its desirable substrate promiscuity. Alternatively, the enzymes could be engineered with higher resting state reduction potential, effectively propping open the electron gate. Many factors tune the reduction potential of heme enzymes, including the environment in the proximal pocket,[5] and the nature of the proximal ligand. The reduction potentials of axial mutants of the heme protein cytochrome *c* span a range of 650 mV, from –390 mV for a Cys/His ligated mutant to +262 for the Met/His variant.[6] Interestingly, the potential of cysteine-ligated cytochrome *c* (–390 mV) is similar to that of P450. Replacement of the strong, axial thiolate with a weakly donating water molecule results in a positive shift of almost 350 mV.

To this end, the Arnold group designed a second generation of mutants in which the axial cysteine ligand (C400) is replaced with other amino acids, including serine. It was hypothesized that the more weakly donating serine ligand would result in a positive shift in reduction potential, similar to the observations for cytochrome *c*. As described in Chapter 1, cysteine ligation is critical for the activation of dioxygen and generation of the ferryl porphyrin radical active species known as compound I (**Figure 6.3** left, highlighted green).[7] Mutation of the axial cysteine to serine in mammalian P450s abolishes monooxygenation activity.[8] However, this ligation was not expected to be necessary for cyclopropanation, as free hemin also catalyzes this reaction.

This is in fact the case; serine-ligated P450 BM3 mutants are highly active for cyclopropanation reactions, and show selectivity for cyclopropanation over epoxidation of styrene, even under aerobic conditions (**Figure 6.4**, right).[9] The Arnold group chose to examine one mutant in particular, which contains 13 mutations to the active site and periphery and the C400S mutation. This mutant catalyzes over 300 turnovers *in vitro*, and is characterized by a ferrous-CO species with an absorbance max at 411 nm.[9] For the purposes of this Chapter, this particular mutant will be referred to as $P411_{13}$-Ser. The serine-ligated P450-BM3 heme domain (C400S) has been characterized by X-ray crystallography, which indicates serine-ligation of the heme active site (**Figure 6.4**, left).

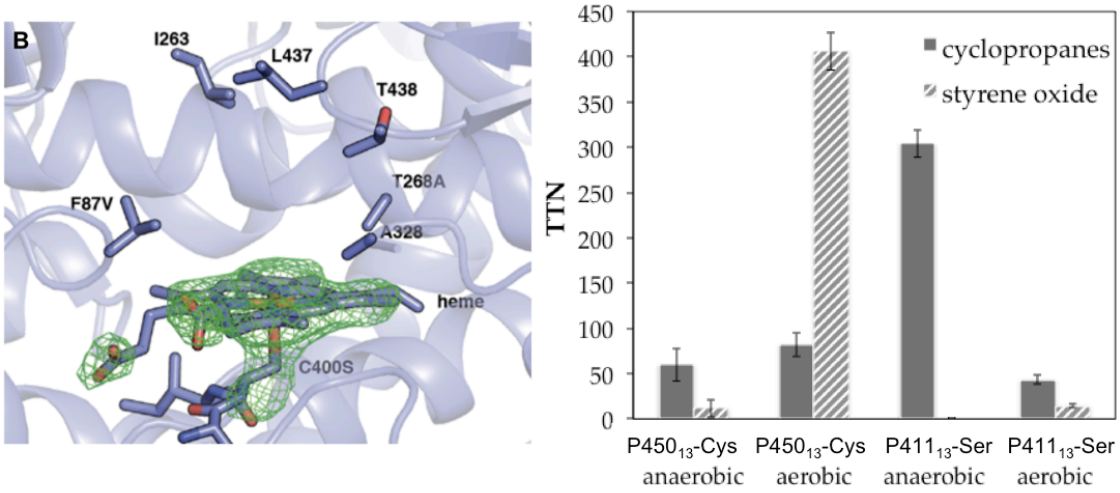

Figure 6.4. $P411_{13}$-Ser structure and activity.[9] **Left**: electron density maps show serine ligation to the heme of $P411_{13}$-Ser heme domain. **Right**: Total turnover numbers (TTN) for P450-catalyzed reactions.

The central question for the function of this catalyst, and improvement to future catalysts is: Does the cysteine-to-serine mutation in P450 also result in a positive shift in reduction potential? Furthermore, is this shift sufficient to make reduction by NADH and flavin cofactors thermodynamically favorable?

Determination of reduction potentials is difficult for enzymes such as P450s. Standard voltammetry techniques are fraught with challenges, including slow diffusion of the large proteins, and poor communication between the buried heme and the working electrode. Additionally, the ferrous state of cytochrome P450 is extremely sensitive to oxygen, and readily auto-oxidizes to ferric. Any method to determine P450 $E°'(Fe^{III/II})$ must be done under strictly anaerobic conditions.

Various methods exist for determining reduction potentials, including spectrophotometric titrations, spectroelectrochemical titrations, potentiometric titrations, and direct electrochemistry of immobilized or freely-diffusing enzymes. However, these techniques result in a wide range of reported potentials. For example, a range of potentials from –368 mV to –427 mV are reported for solution measurements of wild-type (WT),[5,10] substrate free P450 BM3. Protein film voltammetry has led to even more positive reported values of approximately –133 to +4 mV.[10–12] Careful determination of solution reduction potentials and internal comparison between wild type and mutant enzymes is needed.

This Chapter reports the measurement of ferric/ferrous reduction potentials for a variety of P450 mutants. It also describes the advantages and limitations of various techniques that may be used to determine solution ferric/ferrous reduction potentials for P450 variants. In particular, we address whether the ligation change results in a shift in reduction potential within range of biological reductants (NADH, FMN). Unless specified otherwise, all potentials are measured at neutral pH, and are reported versus the normal hydrogen electrode (NHE).

Enzymes

In order to avoid complications with the optically- and redox-active flavin cofactors, all measurements use only the heme domains of all P450 BM3 mutants,

rather than the holo enzyme. To test titration methods and provide an internal reference for reduction potentials, we have examined WT enzymes P450 BM3, and CYP119 from *Sulfolobus acidocaldarius*. To probe the effect of axial ligation on $E°'(Fe^{III/II})$, we examined BM3 axial mutants: C400S, C400M, C400H, C400Y, C400A, and C400D. We also examined two mutants specifically engineered for cyclopropanation activity. The first mutant, which will be referred to as $P450_{13}$-Cys, contains the 13 mutations V78A, F87V, P142S, T175I, A184V, S226R, H236Q, E252G, T268A, A290V, L353V, I366V and E442K (**Figure 6.5**). The second mutant, $P411_{13}$-Ser, is identical to $P450_{13}$-Cys except that it contains C400S serine ligation.

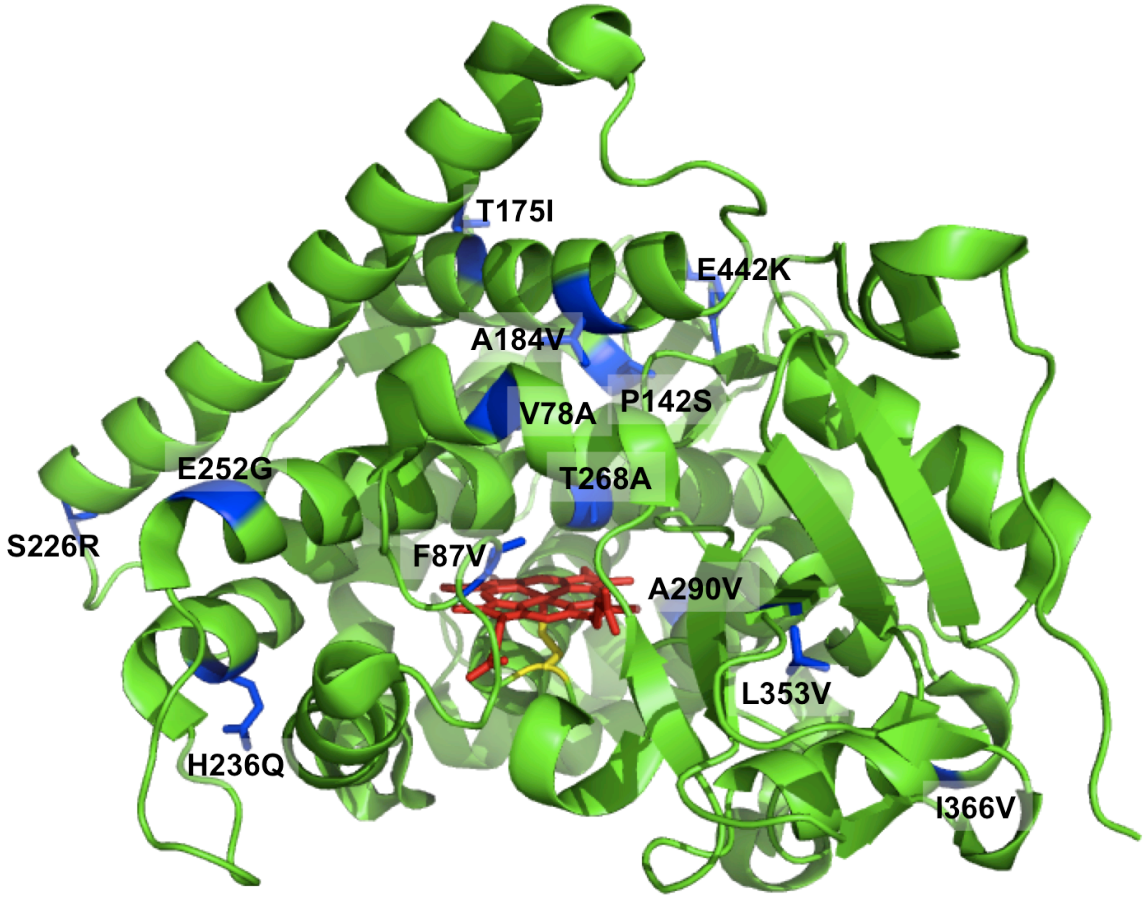

Figure 6.5. Structure of $P450_{13}$-Cys, highlighting mutations in blue (PDB 4H23).

6.2. Methods Development for Redox Titrations

Spectrophotometric Titration

Spectrophotometric titrations present an experimentally straightforward means to determine reduction potentials. An enzyme sample is titrated by addition of chemical oxidant/reductant of known potential, and absorption spectra are acquired at each point along the titration. Absolute concentrations of reduced and oxidized species are determined based on the absorption profile, to determine K_{eq} (Equation 6.1). The enzyme reduction potential is determined using Equation 6.3, where $\Delta E°$ is the reduction potential of the enzyme, and ΔE is the difference in potentials between the enzyme and titrant.

For a reaction: $Enz(ox) + A(red) \rightarrow Enz(red) + B(ox)$

$$K_{eq} = \frac{[Enz(red)][B(ox)]}{[Enz(ox)][A(red)]} \tag{6.1}$$

$$\Delta G° = -RT \ln K_{eq} = -nF\Delta E° \tag{6.2}$$

$$\Delta E = \Delta E° - \frac{RT}{nF} \cdot \ln\left(\frac{[Enz(red)][B(ox)]}{[Enz(ox)][A(red)]}\right) \tag{6.3}$$

The requirements for this method are: 1) Enzyme, in which the reduced and oxidized forms of the protein have distinct absorption profiles with known extinction coefficients; 2) A chemical oxidant/reductant with a known reduction potential within ~100 mV of the enzyme, and in which the reduced and oxidized forms have distinct absorption profiles with known extinction coefficients. Advantages of this method are that low concentrations and volumes of protein can be employed, and no specialized equipment is necessary, other than a

spectrophotometer and cuvette under anaerobic atmosphere (e.g., within a glovebox).

As discussed previously, the $E°'(Fe^{III/II})$ for WT P450 BM3 is expected to fall within the range of –365 to –430 mV. Methyl viologen radical cation ($MV^{+\bullet}$) was chosen as the chemical reductant; this species has strong absorbance in the visible region (**Figure 6.6**), and its reduction potential $E°'(MV^{2+}/MV^{+\bullet})$ = –446 mV[13,14] falls within 100 mV of the expected P450 potential. $MV^{+\bullet}$ can be generated from MV^{2+} dichloride, which is optically transparent, by mixing an aqueous MV^{2+} solution with zinc powder under anaerobic conditions.[15] The radical reacts quickly with oxygen to regenerate MV^{2+}; however, under anaerobic conditions, it is stable for many hours.[16]

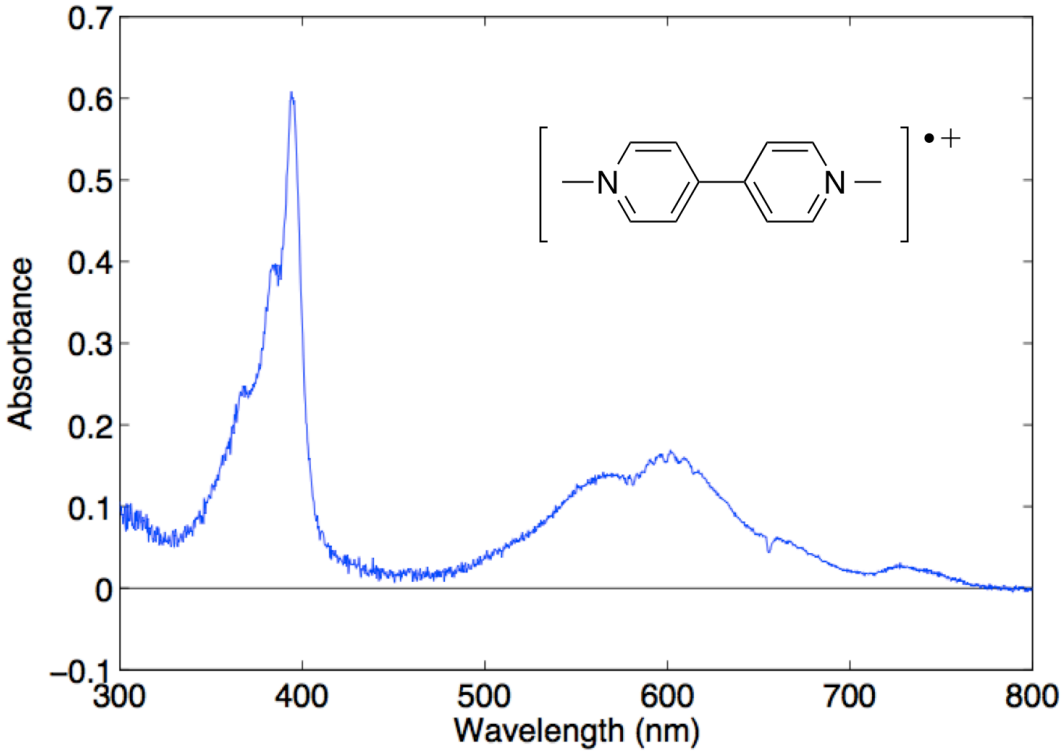

Figure 6.6. Absorption spectrum of the methyl viologen radical cation. Reduction was accomplished by mixing over zinc powder in a glovebox.

Addition of aliquots of $MV^{\bullet+}$ to a solution of ferric, WT P450 results in a series of titration spectra, shown in **Figure 6.7**. There is significant overlap between the $MV^{\bullet+}$ and P450 absorbance spectra in the range of 350-600 nm; this makes spectral deconvolution more difficult.

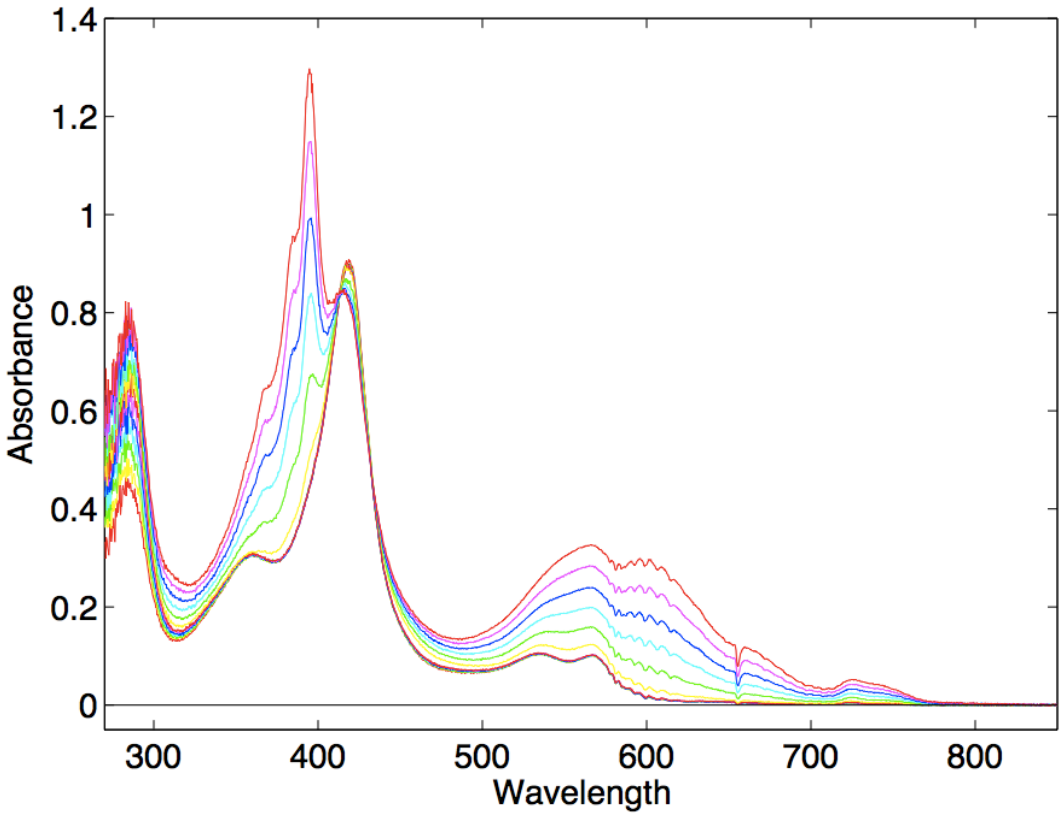

Figure 6.7. Chemical titration of WT P450 BM3 with $MV^{\bullet+}$.

There are other significant concerns with regards to the success of these titrations. Importantly, trace amounts of oxygen can affect the data. Oxygen reacts rapidly with both the ferrous P450 and with $MV^{\bullet+}$. This adds a third redox couple to the reaction, yet there are no optical signals to indicate the concentration of oxygen, or of the oxidized MV^{2+}. It is extremely difficult to remove all traces of oxygen from protein samples; multiple freeze-thaw cycles (e.g., freeze-pump-thaw) or sparging can be detrimental to the protein structure, and therefore, redox properties. There was also a significant amount of error with respect to titrant volumes; the positive

pressure necessary in the glovebox makes accurate pipetting of microliter quantities very difficult. Furthermore, this method requires use of a titrant within ~100 mV of the expected reduction potential. A new titrant would need to be found for each mutant, decreasing the generalizability of the method. For all of these reasons, spectrochemical titrations were abandoned for measurement of P450 BM3 reduction potentials.

Electrochemical titration

Electrochemical titrations require a more complex, experimental setup, but determination of ferric/ferrous P450 concentrations and relevant potentials is more straightforward. In this method, reduction of the enzyme is accomplished using a narrow-pathlength spectroelectrochemistry cuvette, with a three-electrode setup (**Figure 6.8**).

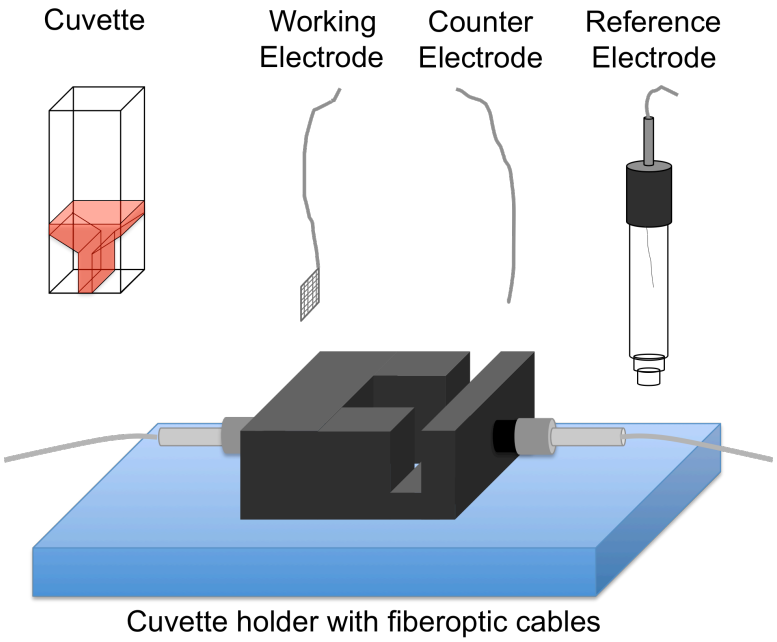

Figure 6.8. Spectroelectrochemical setup. Quartz cuvette with 1mm pathlength, Pt mesh working electrode, Pt wire counter electrode, and AgCl/Ag reference electrode.

When the potential at the electrode approaches the heme reduction potential, electrons flow from the large-surface area working electrode to the P450 heme, relayed via a mixture of small molecule mediators with varying $E°'$ (**Figure 6.9**). After equilibration at each potential, spectra are recorded to determine the relative concentrations of reduced and oxidized enzyme (**Figure 6.10**).

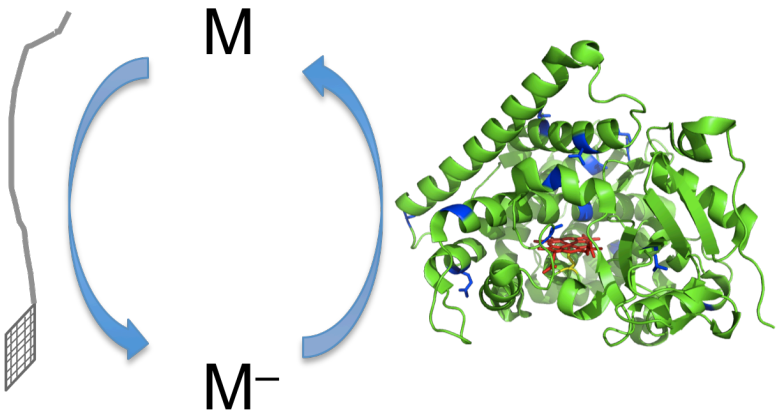

Figure 6.9. Electron relay between the Pt mesh working electrode and the P450 heme (red). "M" represents the small molecule mediators.

For these measurements with short path length (1 mm), the enzyme concentration (~30-70 μM) is greater than that of the mediators. Only the ferric and ferrous P450 species contribute significantly to the visible absorbance spectrum, facilitating spectral deconvolution. A plot of relative $\%Fe^{II}$ versus applied electrode potential can be fit to the one-electron Nernst equation to determine $E°'$ for the enzyme.

We performed a spectroelectrochemical reduction of the WT BM3 heme using the setup described above, applying electrode potentials over a range of –100 to –530 mV (**Figure 6.10**). Following this reduction, an aliquot of sodium dithonite was added to accomplish complete heme reduction, and the analogous, reverse titration (oxidation) was performed (**Figure 6.11**).

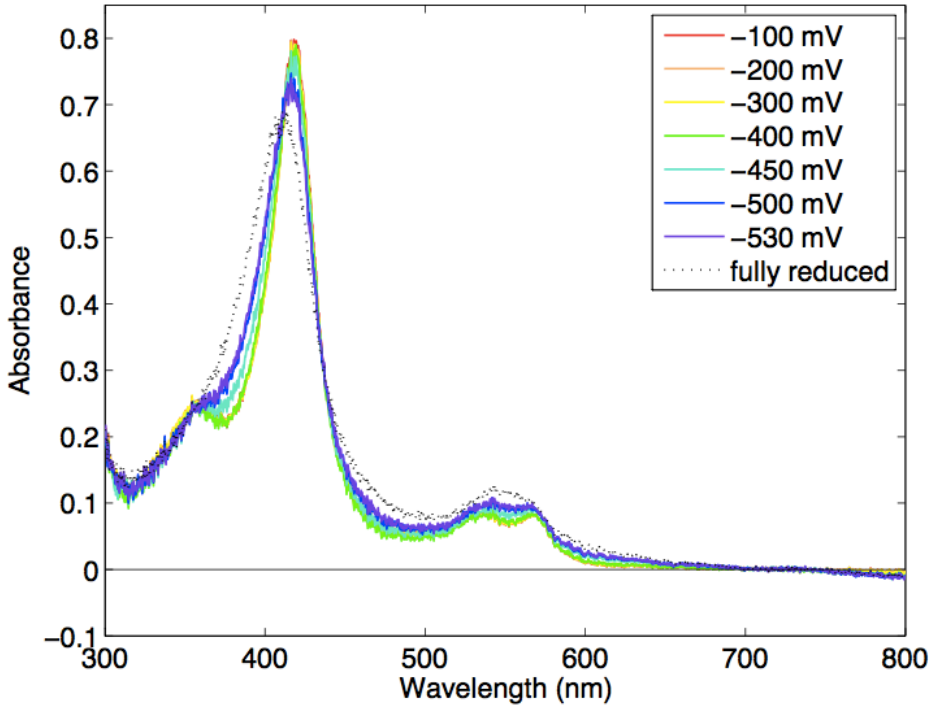

Figure 6.10. Absorption spectra taken during the spectroelectrochemical reduction of WT BM3.

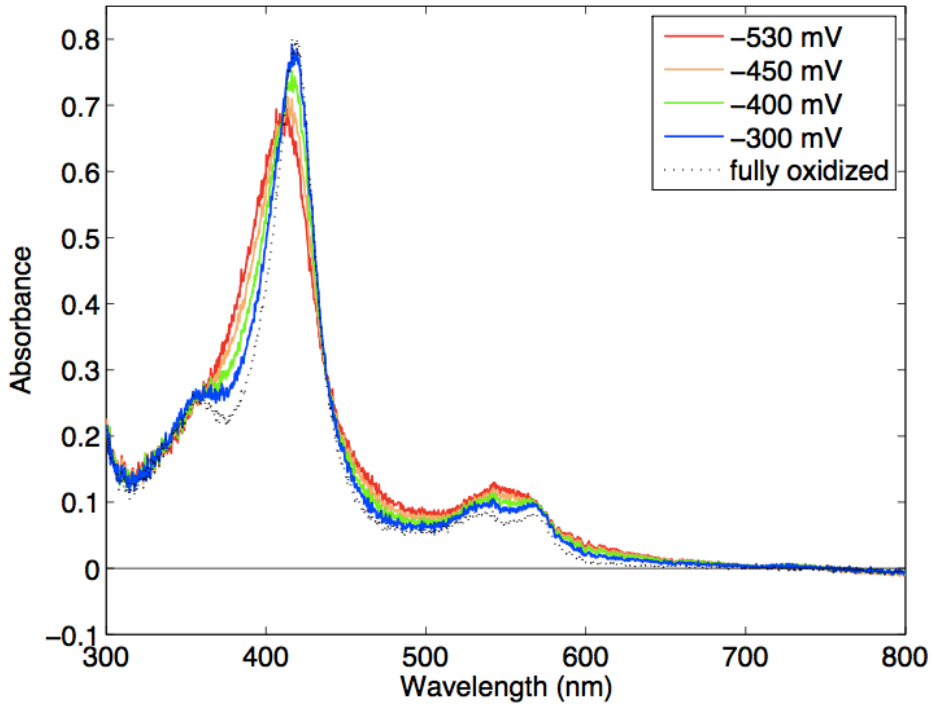

Figure 6.11. Absorption spectra taken during the spectroelectrochemical oxidation of dithionite-reduced WT BM3.

We deconvoluted the spectra (300-600 nm) into ferric and ferrous components using a Matlab program (see Appendix D). A plot of % ferrous P450 versus applied potential is shown in **Figure 6.12**.

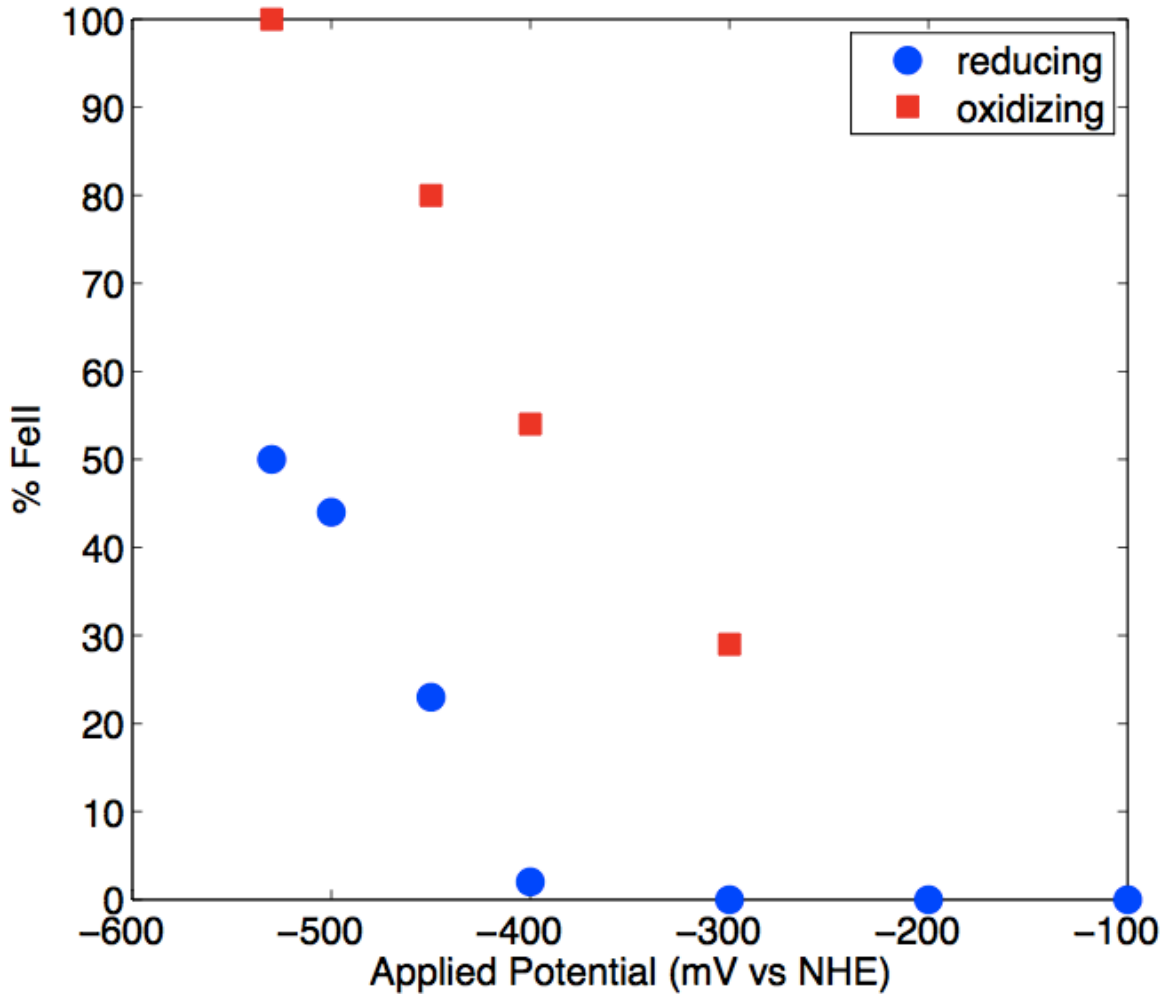

Figure 6.12. Plot of the electrochemical titration of WT BM3. Blue circles: reductive titration. Red squares: oxidative titration.

Significant hysteresis was observed between the reductive and oxidative titrations, making it impossible to fit the data to the Nernst equation. This hysteresis is most likely due to slow equilibration between the electrode and the bulk solution at low concentrations of redox mediators (1-10 μM). Using higher concentrations of

redox mediators is undesirable, as these optically active small molecules interfere with the spectral deconvolution of ferric and ferrous P450 concentrations. Additionally, in these initial experiments (and for space reasons within the spectroelectrochemical cuvette), the counter electrode was not kept in a separate fritted compartment; it is likely that reoxidation/rereduction at the counter electrode precluded full conversion between oxidized and reduced states of the enzyme. For these practical reasons, we have modified this approach, as described below.

Potentiometric titration

Potentiometric titrations are very similar to the electrochemical titrations, except that the supply of reducing/oxidizing equivalents is accomplished by addition of chemical reductants/oxidants. In this case, reduction is accomplished by addition of sodium dithionite, and re-oxidation is accomplished by addition of potassium ferricyanide. The open circuit potential (OCP, potential applied by the electrode at which no current flows) is measured after every chemical addition to determine the solution potential. $\%Fe^{II}$ is again determined by deconvolution of absorption spectra into ferric and ferrous components.

Chemical (rather than electrochemical) reduction/oxidation results in faster equilibration of the sample volume upon manual mixing. For these measurements, the electrode need not be high surface area (in contrast to the spectroelectrochemical titration). A single wire working electrode can be used. The reduction potential of aquo-ligated WT P450 BM3 is fairly negative (vide infra), and approaches the thermodynamic potential for proton reduction (at pH 7). Clean platinum wires begin to evolve hydrogen at the relevant potentials, which

complicates the OCP measurements. Implementation of a gold wire working electrode greatly improved potentiometric titrations.

Test: Wild-type P450 BM3

The spectra during titration with dithionite show clean conversion from ferric to ferrous with multiple isosbestic points (**Figure 6.13**). Reoxidation by ferricyanide also proceeds cleanly (**Figure 6.14**).

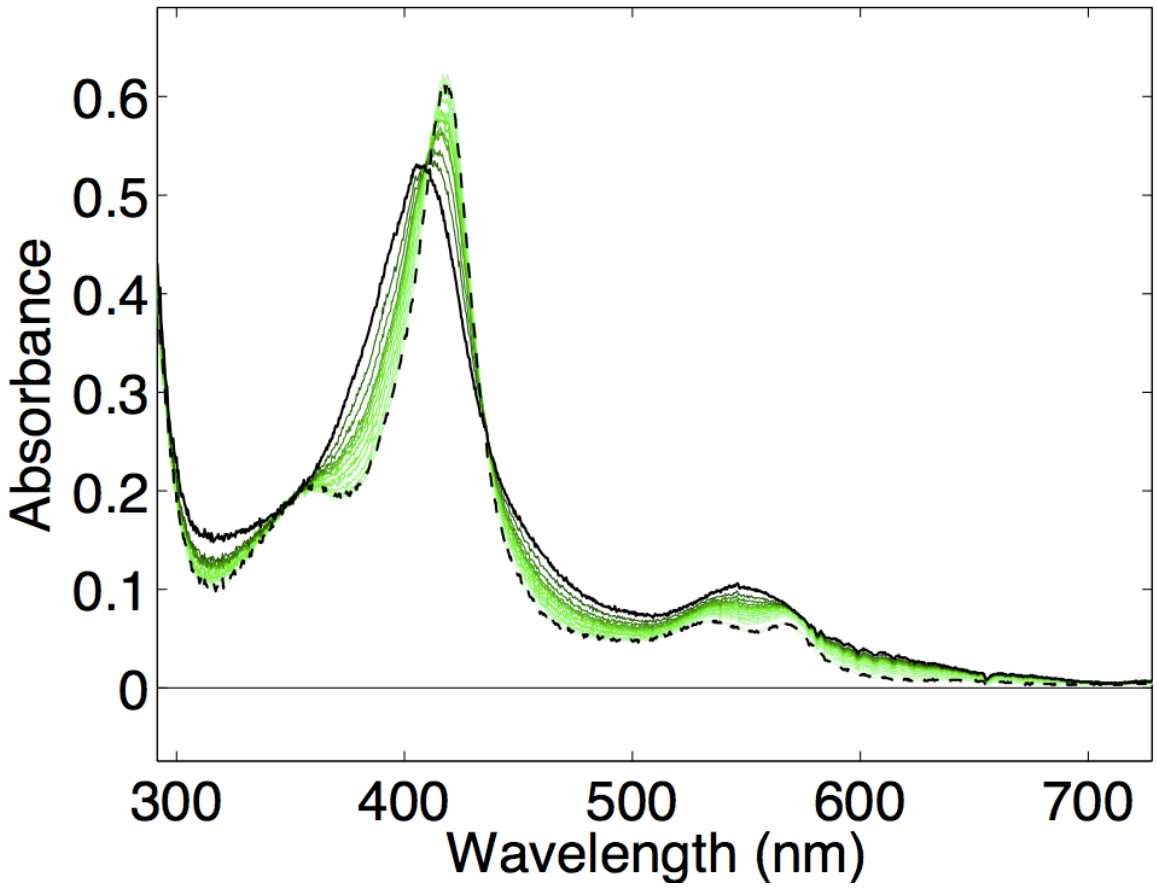

Figure 6.13. Absorption spectra of WT BM3 during reductive potentiometric titration. Ferric: black dashed line. Ferrous: black solid line.

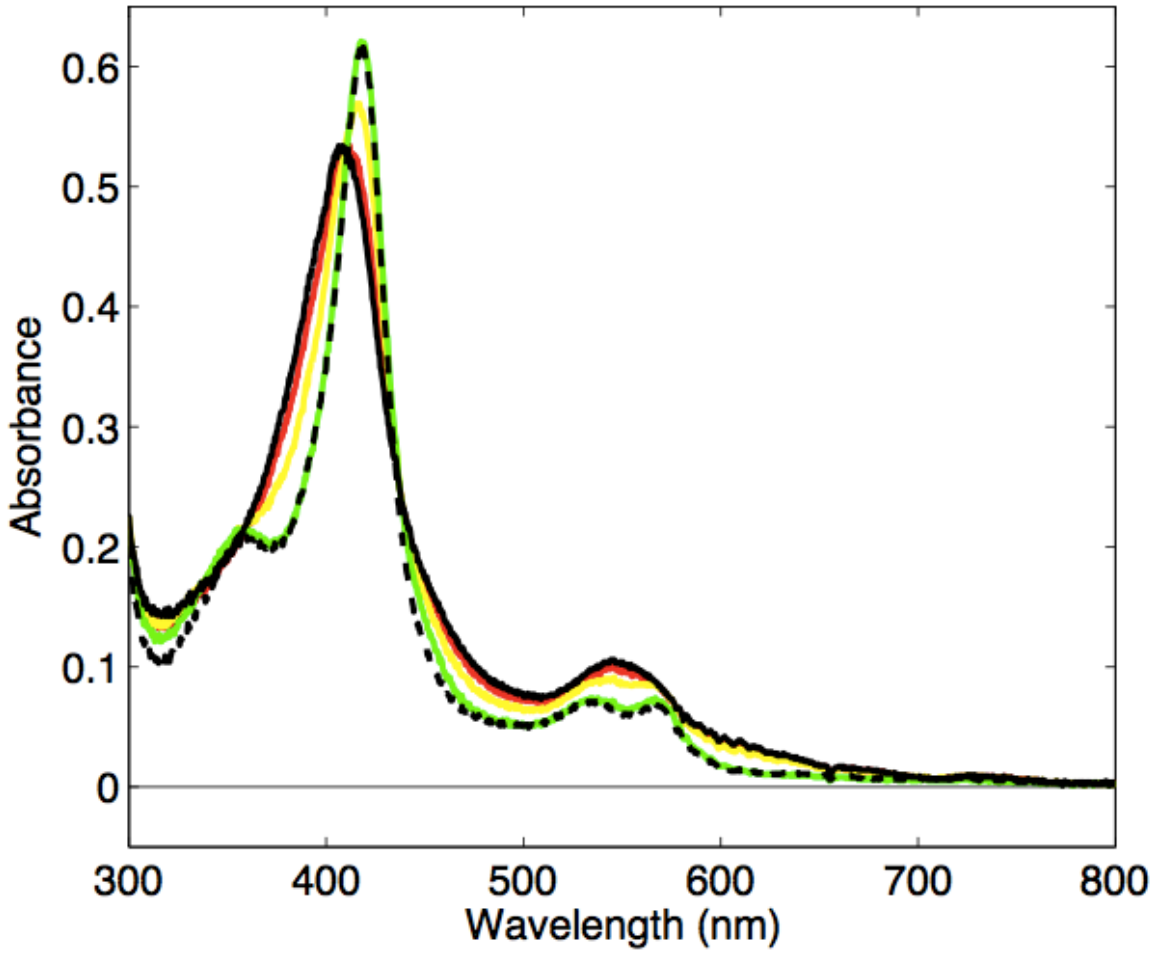

Figure 6.14. Absorption spectra of WT BM3 during oxidative potentiometric titration. Ferrous: black solid line. Ferric (pre-titration): black dashed line.

There is only minor drift in open circuit potentials over the course of the measurement (10 min), almost always toward more positive values (**Figure 6.15**). The drift was generally less than 1.5 mV/min; in cases where drift exceeded this benchmark, an additional 5 minute period was recorded. Excessive amounts of drift (5 mV/min, or more) generally indicated incomplete mixing, the presence of oxygen, sample impurities, or a dirty working electrode. In these cases, manual mixing was repeated, or samples, buffers and electrodes were removed from the box, cleaned/purified and re-deoxygenated, and the titration was attempted again from the beginning.

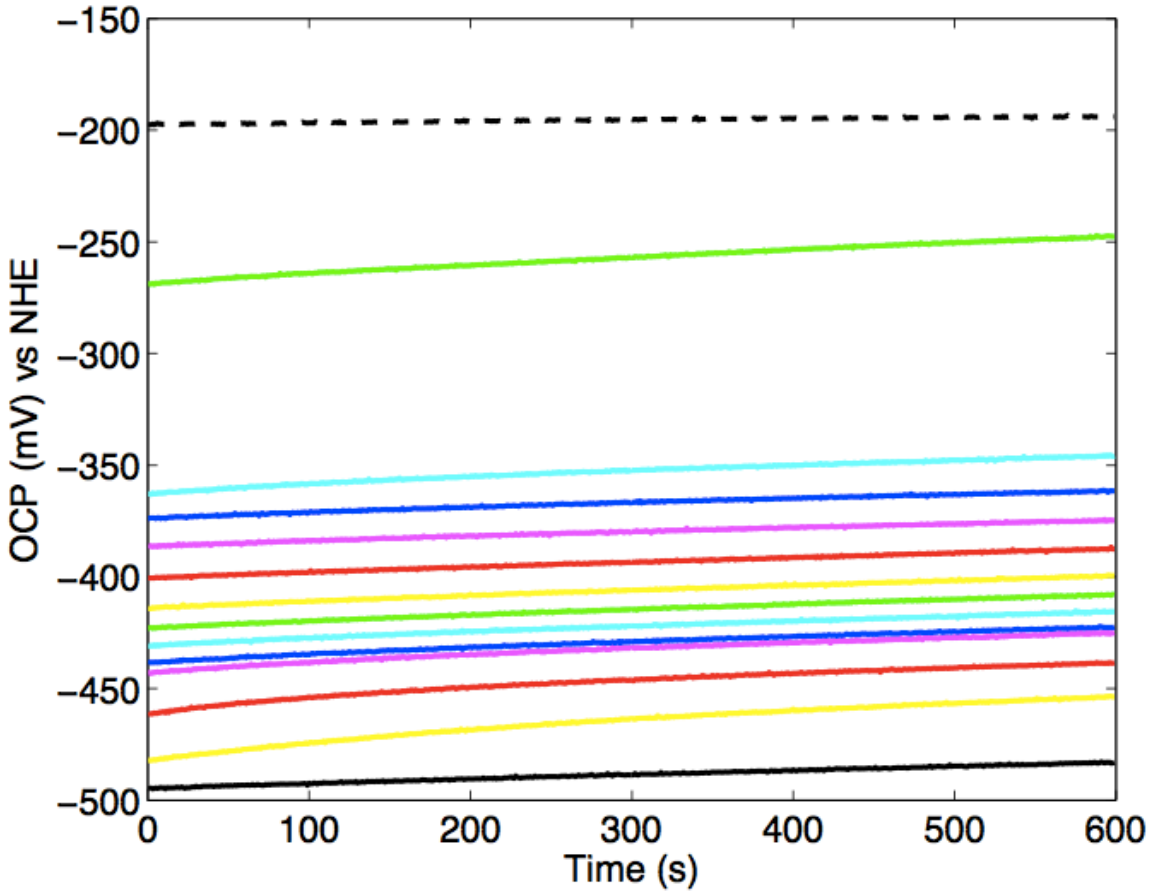

Figure 6.15. Open circuit potential measurements of WT BM3 during potentiometric titration. Dashed black line: first titration point. Solid black line: fully reduced (excess dithionite).

Spectra were deconvoluted to ferric and ferrous components, as discussed previously (see Appendix D). Relative percent ferrous was plotted against the final OCP value at each point in the titration (**Figure 6.16**). No hysteresis is observed between the reductive and oxidative titrations (**Figure 6.16**). An overlay of the one-electron Nernst equation (Equation 6.4) is used to determine reduction potential.

$$E_{cell} = E^{\circ} - \frac{RT}{nF}\left(\frac{[Fe^{II}]}{[Fe^{III}]}\right) \qquad 6.4$$

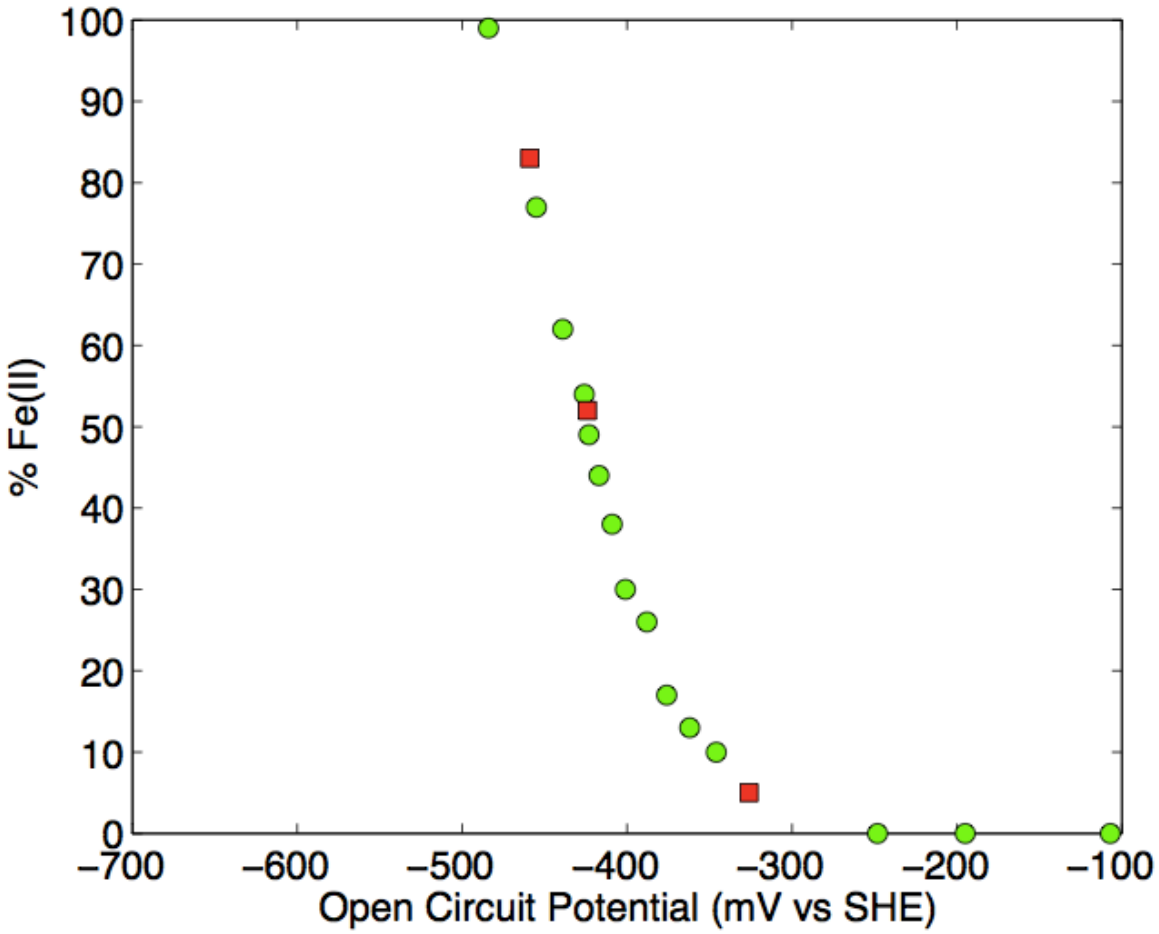

Figure 6.16. Redox titration plot of wild-type P450 BM3. Reduction by sodium dithionite: green circles. Re-oxidation by potassium ferricyanide: red squares.

6.3. Results

6.3.1. Wild-type Enzymes: P450 BM3 and CYP119

Wild Type P450 BM3

The reduction potential for WT P450 BM3 measured by potentiometric redox titration is –420 mV (**Figure 6.17**). This matches closely to the published value of –427 mV.[5] The authors also note that this value agrees with calculations. Most importantly, this value is repeatable, and provides a benchmark with which to compare other mutants (see Appendix C for discussion of errors and repeatability).

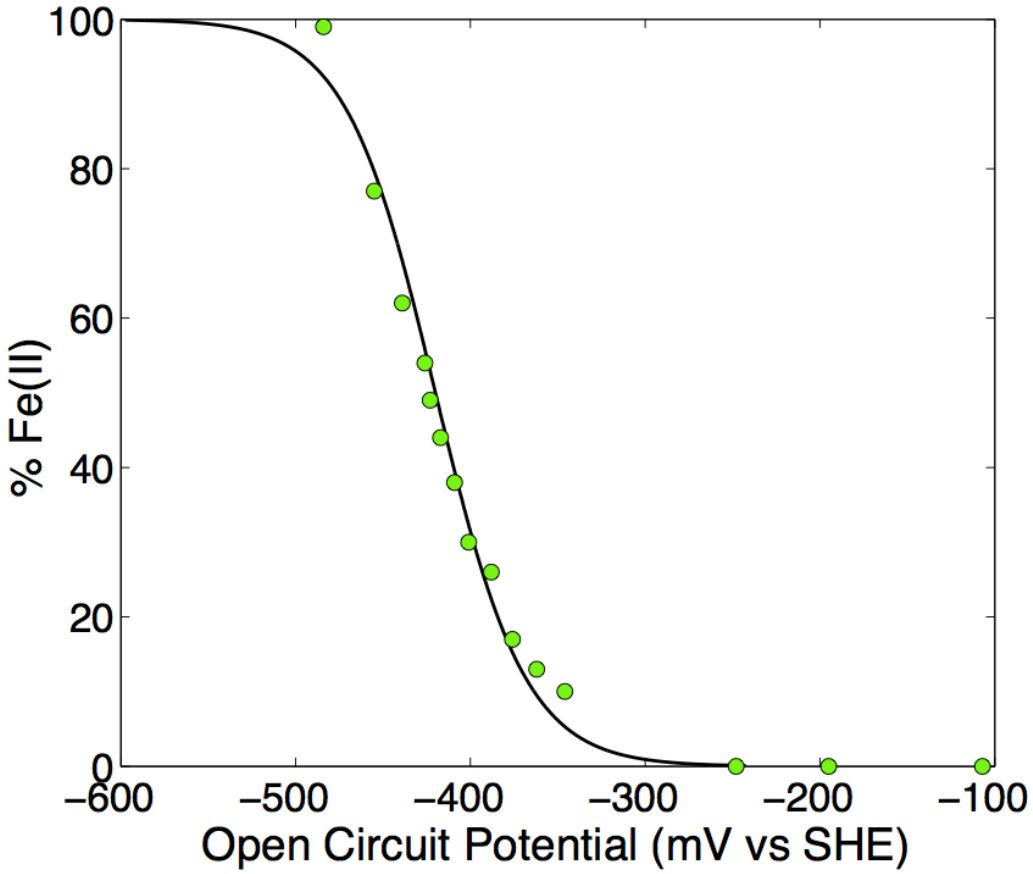

Figure 6.17. Titration curve of WT P450 BM3. The overlayed one-electron Nernst function (black line) has $E°'$=–420 mV.

Wild Type CYP119

We also used this titration method to determine the reduction potential of WT CYP119. The only other report of the WT CYP119 reduction potential, to our knowledge, was determined by protein film voltammetry to be $E°'(Fe^{III/II})$ of –210 mV vs. AgCl/Ag;[17] this corresponds to an anomalously positive value of –10 mV vs. NHE. The same report suggested that CYP119 and myoglobin have the same reduction potential, which is striking as the axial ligation and heme environments of P450 and myoglobin are very different. It is unclear why the CYP119 potential should be 400 mV more positive than other P450s, including P450 BM3.

Potentiometric titration of WT CYP119 with dithionite gives clean conversion from ferric to ferrous, with multiple isosbestic points (**Figure 6.18**). Open circuit potential measurements are stable and consistent (**Figure 6.19**).

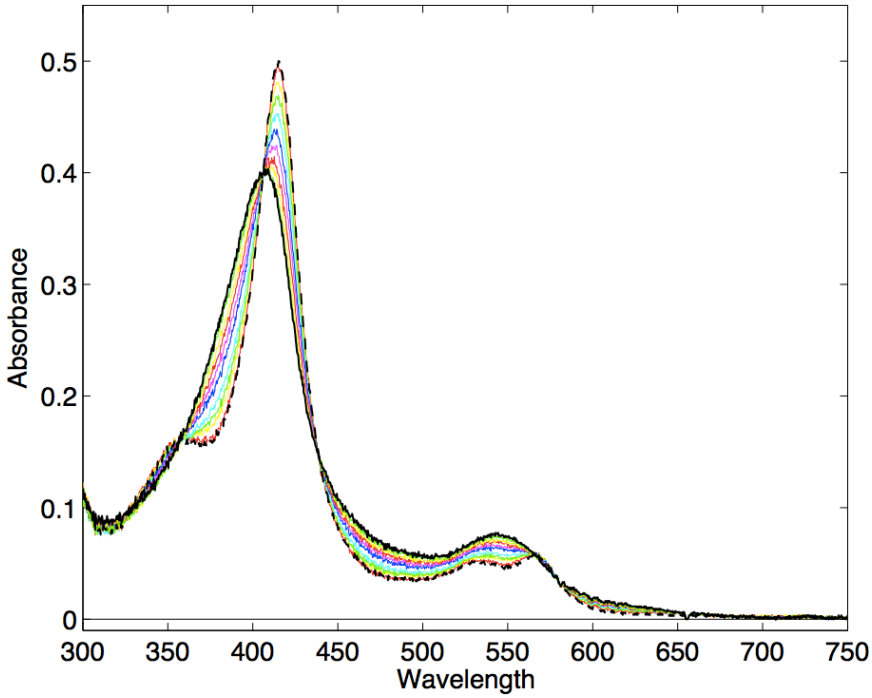

Figure 6.18. Absorbance spectra of WT CYP119 during potentiometric titration with dithionite. Dashed: ferric. Solid black: ferrous.

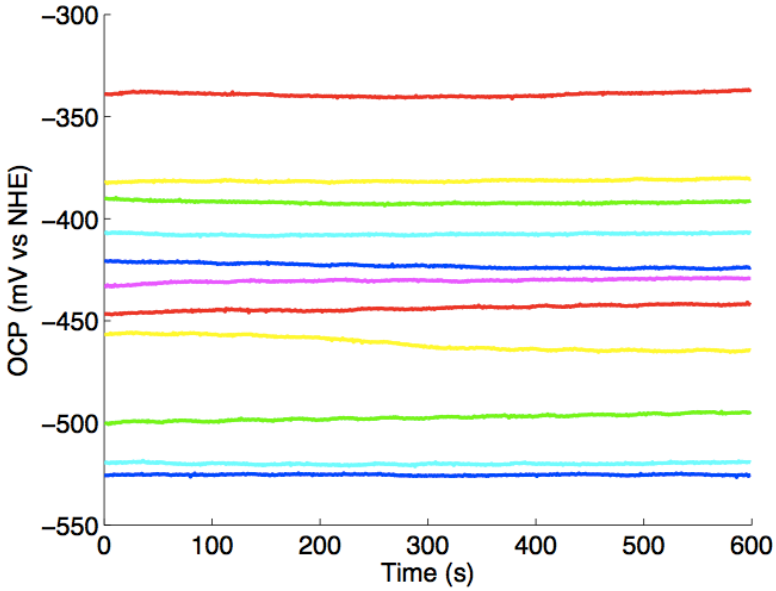

Figure 6.19. Open circuit potential measurements for WT CYP119.

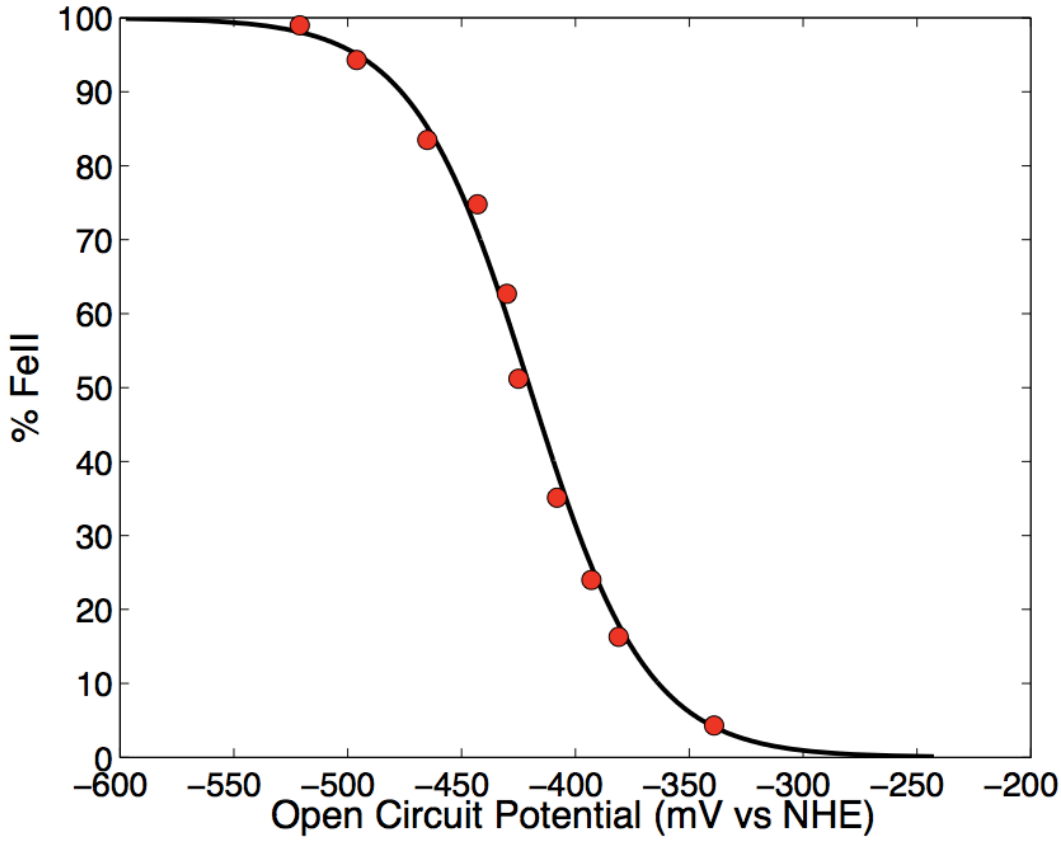

Figure 6.20. Potentiometric titration of WT CYP119 with overlayed Nernst function, $E^{\circ\prime}$ = –420 mV.

The WT CYP119 potential is –420 mV (**Figure 6.20**); this is within error of the value for P450 BM3, and significantly more negative than what was reported by protein film voltammetry.

6.3.2. Potentiometric titration of mutants for *in vivo* cyclopropanation

With a consistent method and reproducible WT BM3 potentials in hand, we set to determine the reduction potentials of P450 BM3 mutants engineered for cyclopropanation. In particular, we were interested in the effect of axial ligation.

C400S axial mutation

The reduction potential of the single mutant C400S was measured by potentiometric titration as described above. Clean isosbestic points are observed in the titration spectra (**Figure 6.21**). The potential for C400S is –290 mV (**Figure 6.22**). This single mutation results in a positive shift of 130 mV compared to WT enzyme, which is sufficient to allow reduction by NAD(P)H.

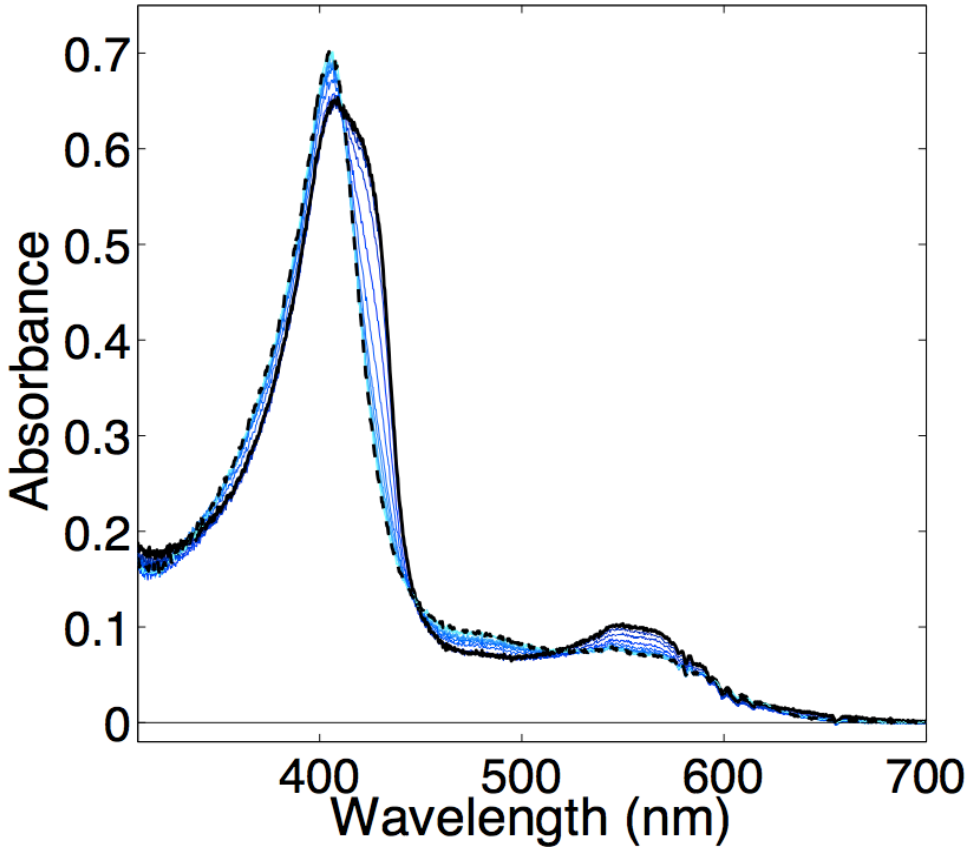

Figure 6.21. Absorption spectra of P450 BM3 C400S. Ferric: dashed; ferrous: solid.

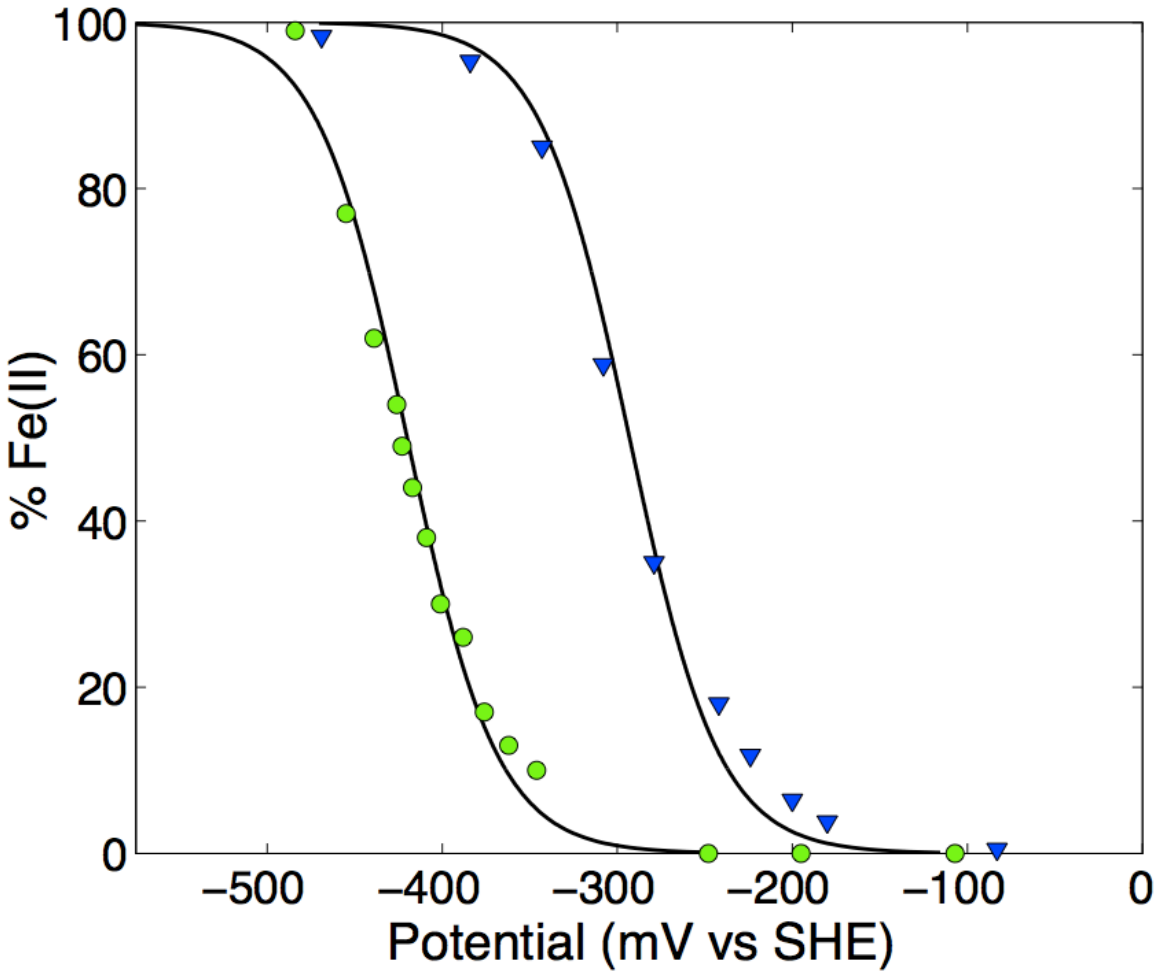

Figure 6.22. Redox titration curves of C400S (blue triangles) and wild-type (green circles), overlayed by the one-electron Nernst function (black line) with $E^{\circ\prime}$ = –420 mV for WT, and –290 mV for C400S.

Engineered cyclopropanation mutants

Reduction potentials were also determined for $P450_{13}$-Cys and $P411_{13}$-Ser (**Figure 6.23**). The 13 mutations to the active site and periphery result in a positive shift of 68 mV from that of WT. Of note, these 13 mutations and the C400S mutation are not additive: $P411_{13}$-Ser is only 148 mV positive of wild type, as opposed to the additive value of 191 mV.

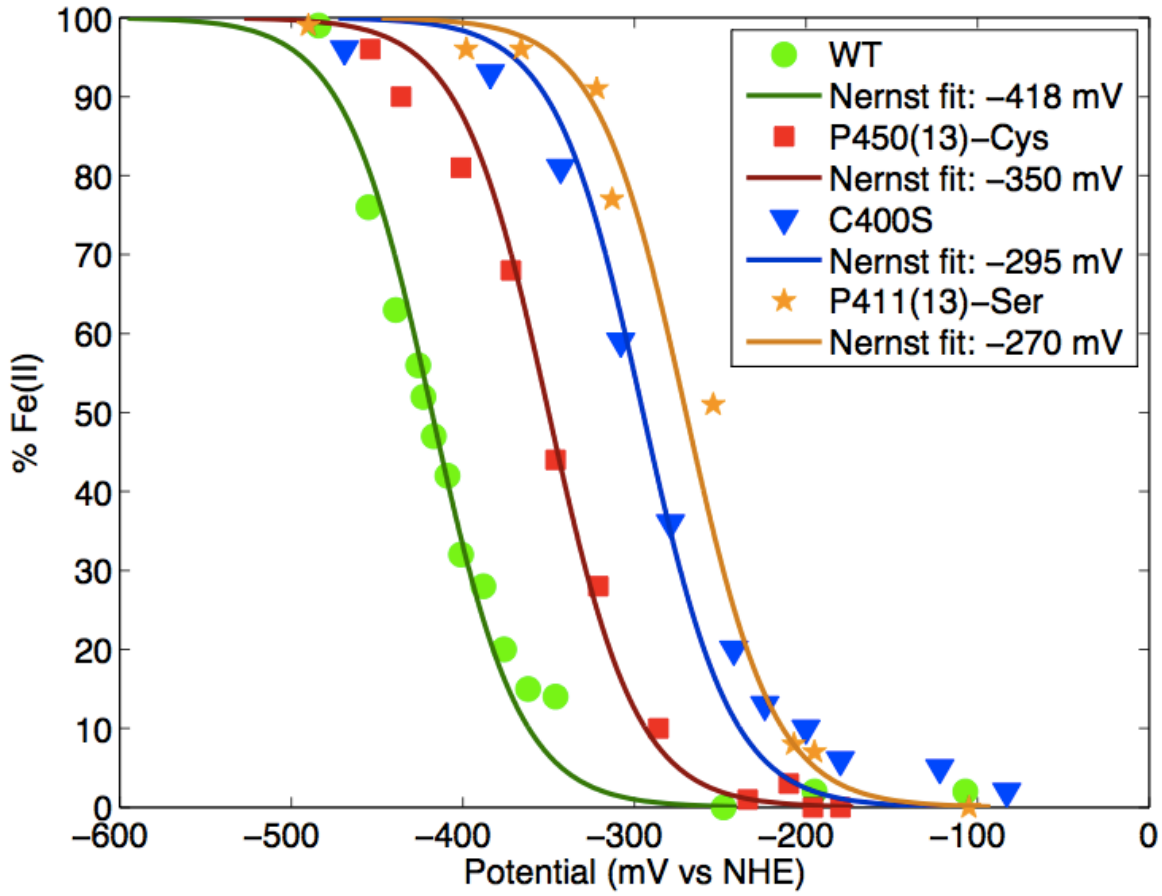

Figure 6.23. Titration curves for four mutants.

6.3.3. Additional axial mutants

The Arnold group also expressed a number of other axial mutants, including: C400M, C400H, C400A, and C400Y.

Titration of C400M yielded a reduction potential of –110 mV (**Figure 6.24).** Somewhat curiously, the titration curve appears to be shallower than the one-electron Nernst function.

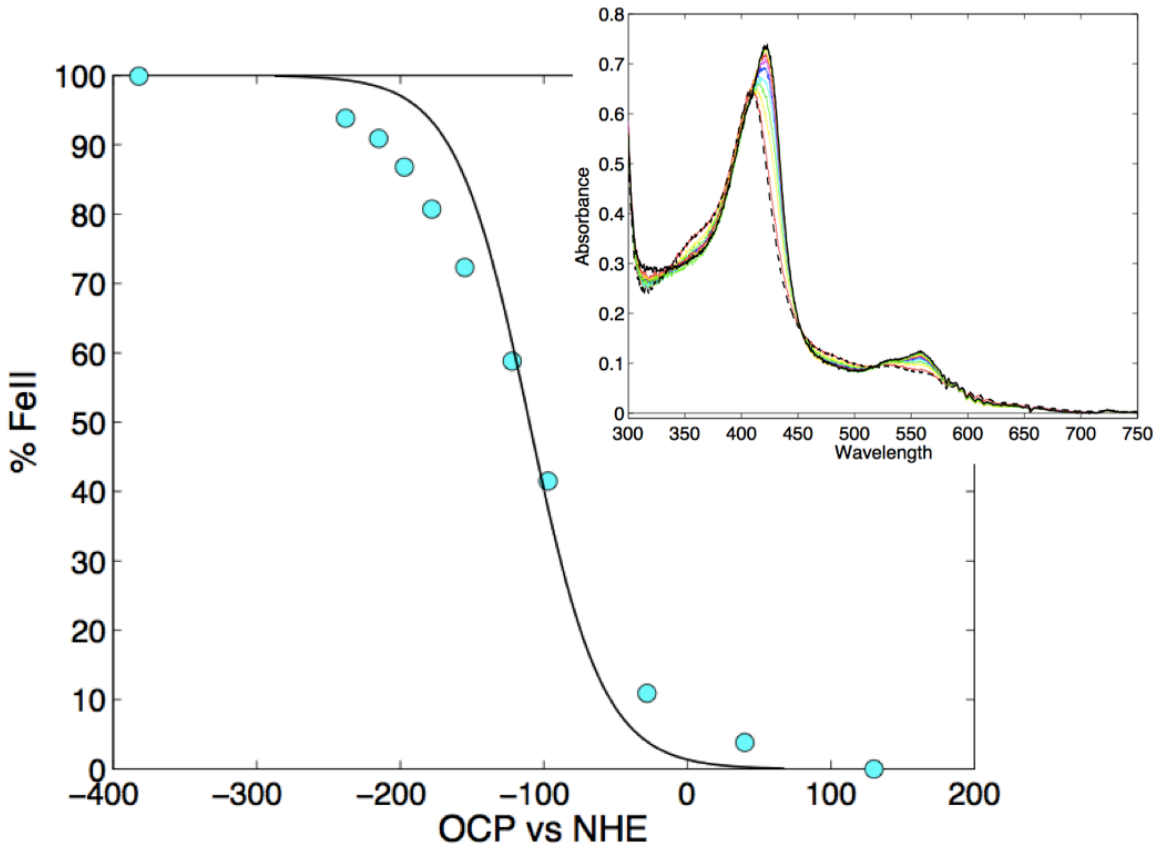

Figure 6.24. Redox titration curve of C400M overlayed by the one-electron Nernst function with $E°'$ = –110 mV(black line). **Inset**: Titration spectra. Dashed: ferric; solid: ferrous.

We also attempted potentiometric titrations of C400H, C400A, C400D, C400Y. Unfortunately, none of these mutants converts cleanly between ferric and ferrous; isosbestic points are not retained, and reoxidation with ferricyanide does not return the initial spectrum (**Figures 6.25-6.28**). These mutants have not been structurally characterized, and electrochemical measurements may be complicated by the presence of impurities, or heterogeneous populations with mixed ligation.

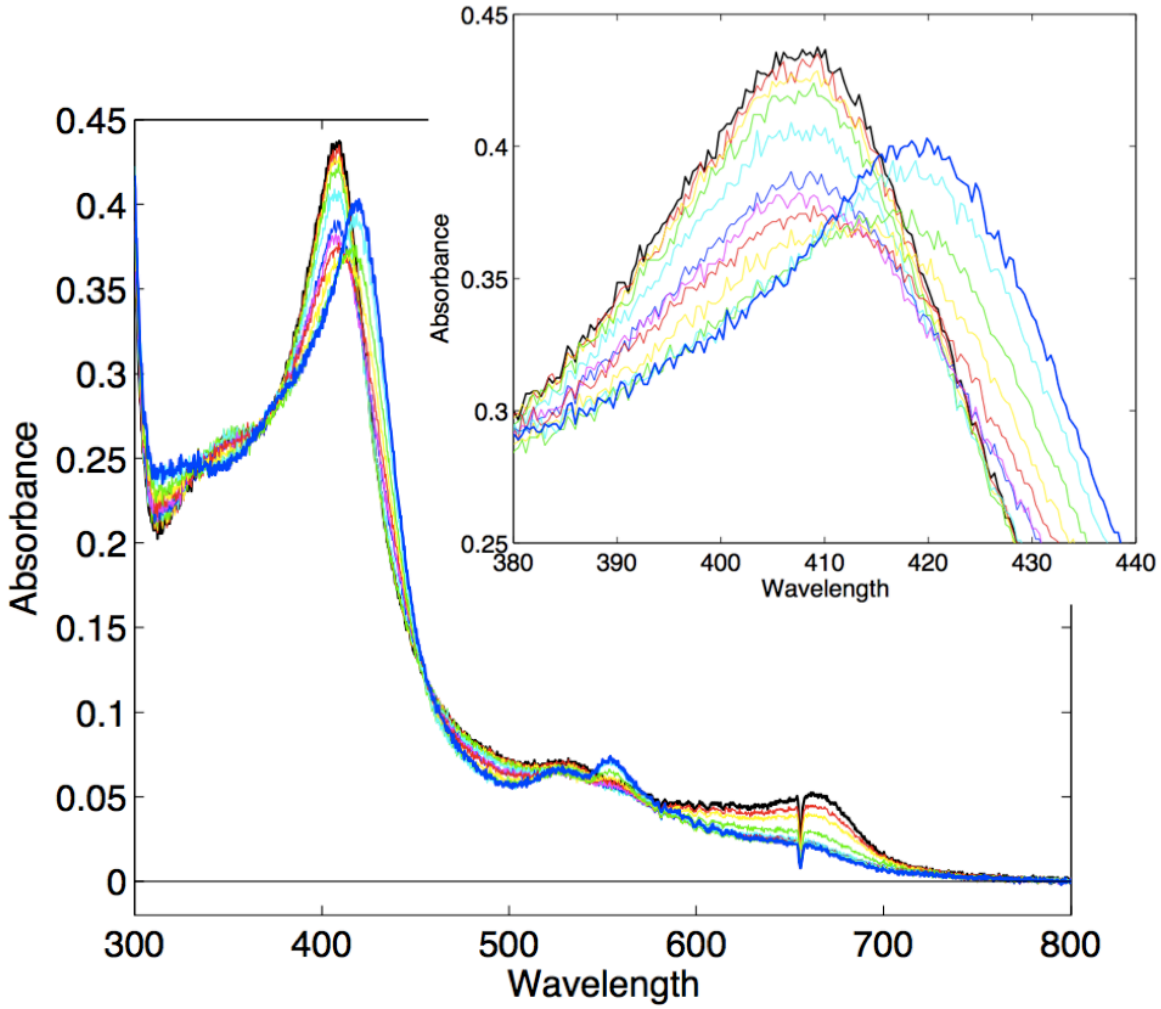

Figure 6.25. Reduction of C400Y shows loss of isosbestic points. Inset: Close-up of Soret region. Ferric: black. Ferrous: dark blue.

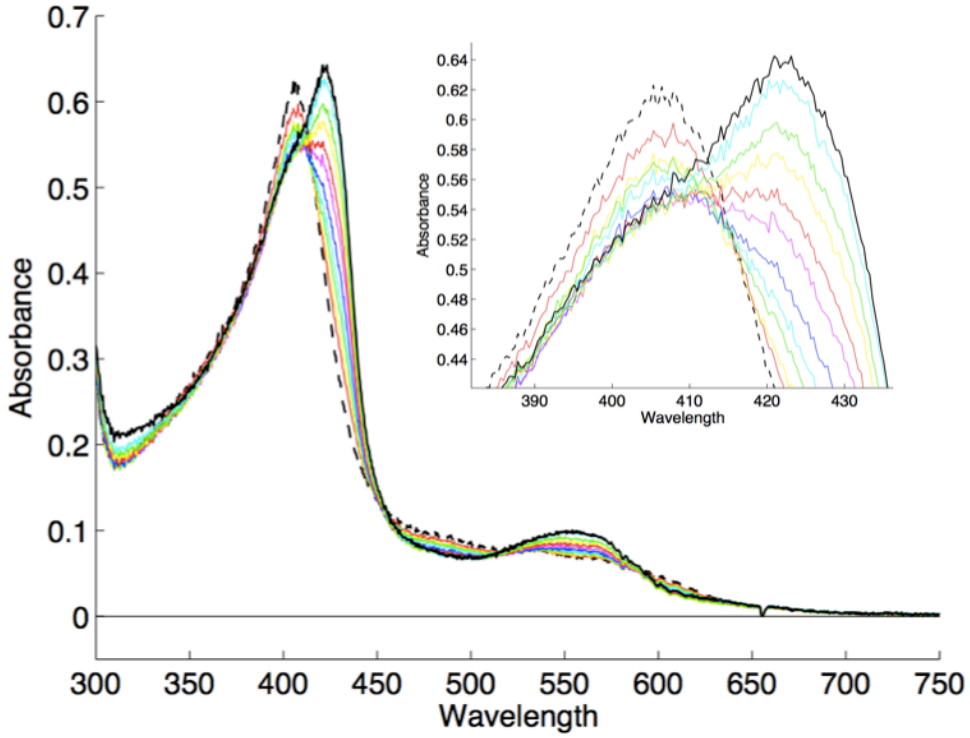

Figure 6.26. Spectra of C400A during potentiometric titration. **Inset**: close-up of Soret region shows non-retention of isosbestic points.

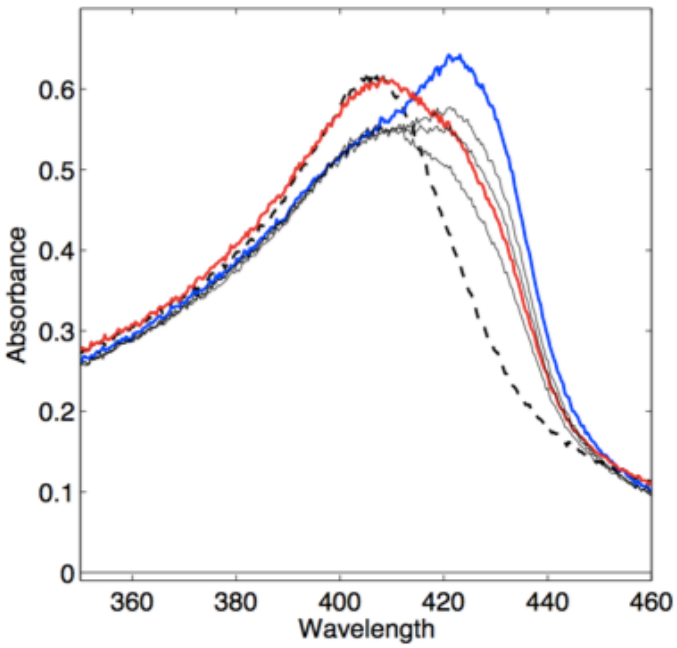

Figure 6.27. Loss of isosbestic points in C400A absorption spectra during titration. Dashed: initial, ferric spectrum. Gray: partial reduction by sodium dithionite. Blue: ferrous spectrum, with excess sodium dithionite. Red: spectrum upon reoxidation with potassium ferricyanide.

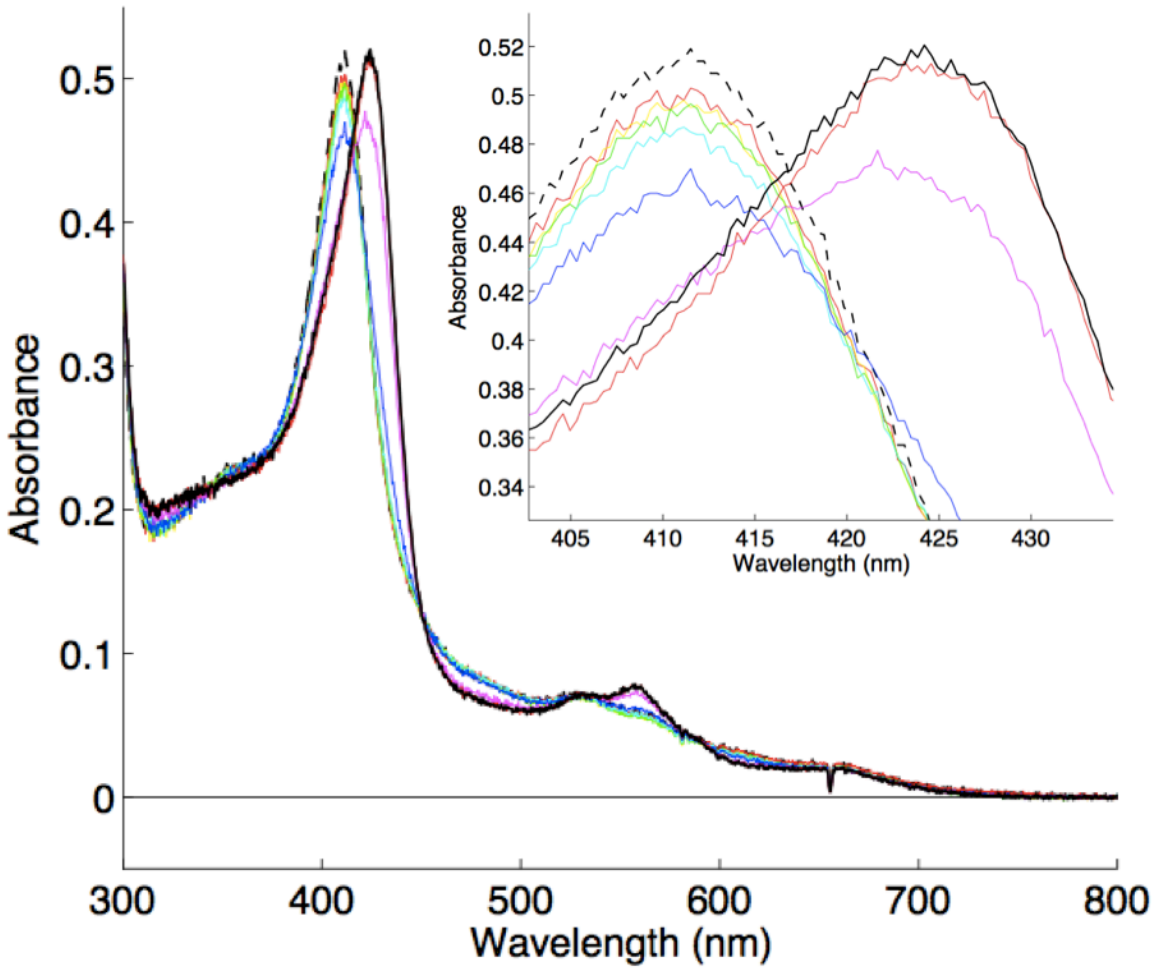

Figure 6.28. Spectra of C400H during potentiometric titration. Inset: close-up of Soret region shows non-retention of isosbestic points.

6.4. Discussion

Using potentiometric redox titration, the reduction potential of wild-type P450 BM3 is –420 mV, in agreement with the more negative reported potential.[5] The engineered cyclopropanation mutant P450$_{13}$-Cys has a more positive potential of –360 mV, however this is still too negative to be efficiently reduced by NADH, relayed through the flavin cofactors (**Table 6.1**). The single axial mutation, C400S, raises the WT reduction potential by 130 mV; this shift the same magnitude as the shift conferred by substrate binding to WT BM3. The engineered mutant P411$_{13}$-

Ser has a similar, positively-shifted reduction potential of –270 mV. Furthermore, this mutant is active in the presence of NADH, and can catalyze cyclopropanation *in vivo*. Whole cell catalysis is capable of generating 27 g/L of cyclopropanes with high enantioselectivity (99% ee_{cis}). *E. coli* cells expressing this mutant can be lyophilized with cryoprotectant and stored for weeks without loss of activity or selectivity.

Table 6.1. Reduction potentials of ferric P450 and redox active cofactors (pH 7)[5,18,19]

Enzyme/Cofactor	$E^{\circ\prime}$ (mV vs. NHE)
NAD^+/NADH ($2e^-$)	–320[a]
FAD/$FADH_2$ ($2e^-$)	–320[b]
FAD/FADH•	–264[b]
FADH•/$FADH_2$	–375[b]
WT BM3 $Fe^{III/II}$	–420 to –440[c,d]
WT BM3 $Fe^{III/II}$ (substrate bound)	–290[c]
WT CYP119 $Fe^{III/II}$	–420[d]
BM3 C400S	–290[d]
BM3 $P450_{13}$-Cys	–360[d]
BM3 $P411_{13}$-Ser	–270[d]
BM3 C400M	–110[d]

a: ref 18. b: ref 19, c: ref 5, d: this work.

6.5. Conclusions and Future Work

We determined the reduction potentials of wild-type and mutant P450 enzymes using potentiometric redox titrations. Among the enzymes analyzed are a series of P450 BM3 mutants designed for cyclopropanation activity. Mutants containing serine-ligation have a formal reduction potential sufficiently positive to allow reduction by endogenously produced NADH, allowing the development of *in vivo*

cyclopropanation. Other mutations in and around the active site that are beneficial for cyclopropanation also affect reduction potentials more positive, but to a lesser degree; the combined axial and active site mutations are not directly additive. Potentiometric titration is limited to highly pure samples that are stable to reduction by dithionite, and accurate potentials cannot be determined for mutants that do not cleanly convert between ferric and ferrous forms.

6.6. Acknowledgments

This Chapter greatly benefited from the guidance and assistance of a number of people. In particular, I would like to thank Dr. James Blakemore for help with initial setup and electrodes; Professor Jeff Warren for assistance regenerating and maintaining the glovebox, providing reference electrodes, suggestions for chemical titrations, discussions for analysis of titration data; Dr. James McKone for fabrication of mesh electrodes and countless discussions for improving electrochemical technique and for interpreting data; Dr. Wes Sattler for suggestions for MV reduction; and Jay Winkler for discussions regarding data analysis and interpretation of reduction potentials. I also must thank all of the above, with the addition of Megan Jackson and Rocio Mercado, for boosting morale during difficult times.

6.7. Materials and Methods

Chemicals

All chemicals were used as received, without further purification. Buffer salts were obtained from J.T. Baker. Sodium dithionite (86%) was obtained from Fluka. Methyl viologen, benzyl viologen, hydroxynaphthoquinone, and potassium

ferricyanide were obtained from Sigma Aldrich. Solutions were prepared using 18 MΩcm water unless otherwise noted.

Instrumentation

Electrochemistry was performed using a WaveNow potentiostat (Pine Research Instrumentation). Spectra were recorded using an Ocean Optics spectrometer (USB2000+).

Procedures

A detailed description of experimental protocols can be found in Appendix B. A brief description of the procedures is given below, highlighting any deviations from the general protocol.

Preparation of samples for redox titration

P450 BM3 mutants supplied by the Arnold group at Caltech. Enzyme samples included: wild type, C400S, C400M, C400Y, C400A, C400H, and $P450_{13}$-Cys, (referred to elsewhere as BM3-CIS: V78A, F87V, P142S, T175I, A184V, S226R, H236Q, E252G, T268A, A290V, L353V, I366V, E442K), $P411_{13}$-Ser (referred to elsewhere as P411-CIS; the same as $P450_{13}$-Cys with an additional mutation: C400S).

Enzyme samples were buffer-exchanged into 100 mM KPO_4, 100 mM KCl, pH 7.4. and deoxygenated via 4 x 20 gentle pump-backfill cycles with argon, with care taken to avoid bubbling.

Water was sparged for 2-3 hours, followed by three cycles of freeze-pump-thaw in an ice/salt/water bath (–10 °C). Pre-weighed, dry salts (buffers, mediators) were

pumped into the glovebox, and stock solutions were prepared by addition of deoxygenated water in the anaerobic atmosphere glovebox. To verify buffer pH, a small sample was removed from the glovebox and measured by pH meter. Dithionite solutions were made fresh (within the box) for each titration, and potassium ferricyanide solutions were remade every few days.

Protein samples consisted of approximately 600 μL of 50-100 μM enzyme with the following mediators added to ensure electrochemical communication between the protein and electrode: 4 μM methyl viologen (MV), 8 μM benzyl viologen (BzV), 12 μM 2-hydroxy-1,4-naphthaquinone.

Potentiometric redox titration

Enzyme samples were titrated by addition of ~2 μL aliquots of 1-4 mM sodium dithionite stock. The open circuit potential (OCP) of the cell was monitored over a 10-min equilibration period; if the drift was more than 15 mV/ 10 min, the OCP was monitored for an additional 5-10 minutes (or until stable). The final OCP value was used to construct the titration curve. Absorption spectra were recorded at the beginning and end of each OCP measurement to assess enzyme stability; the latter spectrum was used to construct the titration curve. Each spectrum was vertically adjusted to achieve zero baseline in the 750-800 nm region (ΔA_{adjust} < 0.015 OD). Percent Fe(II) was achieved by using a Matlab script (see Appendix D). The midpoint potential was determined by least-squares fitting to a single one one-electron Nernst curve.

6.8. References

(1) Munro, A. W.; Daff, S.; Coggins, J. R.; Lindsay, J. G.; Chapman, S. K. Probing Electron Transfer in Flavocytochrome P-450 BM3 and Its Component Domains. *Eur. J. Biochem.* **1996**, *239*, 403–409.

(2) Miles, J. S.; Munro, A. W.; Rospendowski, B. N.; Smith, W. E.; McKnight, J.; Thomson, A. J. Domains of the Catalytically Self-Sufficient Cytochrome-P-450 BM-3 - Genetic Construction, Overexpression, Purification and Spectroscopic Characterization. *Biochem. J.* **1992**, *288*, 503–509.

(3) Coelho, P. S.; Brustad, E. M.; Kannan, A.; Arnold, F. H. Olefin Cyclopropanation via Carbene Transfer Catalyzed by Engineered Cytochrome P450 Enzymes. *Science* **2013**, *339*, 307–310.

(4) Sanders, J. K. M.; Bampos, N.; Clyde-Watson, Z.; Darling, S. L.; Hawley, J. C.; Kim, H.-J.; Mak, C. C.; Webb, S. J. Axial Coordination Chemistry of Metalloporphyrins. In *Inorganic, Organometallic and Coordination Chemistry*; The Porphyrin Handbook; Academic Press: San Diego, CA, 2000; Vol. 3, pp. 1–48.

(5) Ost, T. W. B.; Miles, C. S.; Munro, A. W.; Murdoch, J.; Reid, G. A.; Chapman, S. K. Phenylalanine 393 Exerts Thermodynamic Control over the Heme of Flavocytochrome P450 BM3. *Biochemistry* **2001**, *40*, 13421–13429.

(6) Raphael, A. L.; Gray, H. B. Semisynthesis of Axial-Ligand (position-80) Mutants of Cytochrome-C. *J. Am. Chem. Soc.* **1991**, *113*, 1038–1040.

(7) Dawson, J. H. Probing Structure-Function Relations in Heme-Containing Oxygenases and Peroxidases. *Science* **1988**, *240*, 433–439.

(8) Vatsis, K. P.; Peng, H. M.; Coon, M. J. Replacement of Active-Site Cysteine-436 by Serine Converts Cytochrome P4502B4 into an NADPH Oxidase with Negligible Monooxygenase Activity. *J. Inorg. Biochem.* **2002**, *91*, 542–553.

(9) Coelho, P. S.; Wang, Z. J.; Ener, M. E.; Baril, S. A.; Kannan, A.; Arnold, F. H.; Brustad, E. M. A Serine-Substituted P450 Catalyzes Highly Efficient Carbene Transfer to Olefins in Vivo. *Nat. Chem. Biol.* **2013**, *9*, 485–487.

(10) Daff, S. N.; Chapman, S. K.; Turner, K. L.; Holt, R. A.; Govindaraj, S.; Poulos, T. L.; Munro, A. W. Redox Control of the Catalytic Cycle of Flavocytochrome P450 BM3. *Biochemistry* **1997**, *36*, 13816–13823.

(11) Fleming, B. D.; Tian, Y.; Bell, S. G.; Wong, L.-L.; Urlacher, V.; Hill, H. A. O. Redox Properties of Cytochrome P450BM3 Measured by Direct Methods. *Eur. J. Biochem.* **2003**, *270*, 4082–4088.

(12) Udit, A. K.; Hill, M. G.; Gray, H. B. Electrochemistry of Cytochrom eP450 BM3 in Sodium Dodecyl Sulfate Films. *Langmuir* **2006**, *22*, 10854–10857.

(13) Michaelis, L.; Hill, E. S. The Viologen Indicators. *J. Gen Physiol.* **1933**, *16*, 859–873.

(14) Wardman, P. Reduction Potentials of One-Electron Couples Involving Free-Radicals in Aqueous-Solution. *J. Phys. Chem. Ref. Data* **1989**, *18*, 1637–1755.
(15) Peon, J.; Tan, X.; Hoerner, J. D.; Xia, C.; Luk, Y. F.; Kohler, B. Excited State Dynamics of Methyl Viologen. Ultrafast Photoreduction in Methanol and Fluorescence in Acetonitrile. *J. Phys. Chem. A* **2001**, *105*, 5768–5777.
(16) Chitose, N.; LaVerne, J. A.; Katsumura, Y. Effect of Formate Concentration on Radical Formation in the Radiolysis of Aqueous Methyl Viologen Solutions. *J. Phys. Chem. A* **1998**, *102*, 2087–2090.
(17) Immoos, C. E.; Chou, J.; Bayachou, M.; Blair, E.; Greaves, J.; Farmer, P. J. Electrocatalytic Reductions of Nitrite, Nitric Oxide, and Nitrous Oxide by Thermophilic Cytochrome P450 CYP119 in Film-Modified Electrodes and an Analytical Comparison of Its Catalytic Activities with Myoglobin. *J. Am. Chem. Soc.* **2004**, *126*, 4934–4942.
(18) Harris, D. C. *Quantitative Chemical Analysis*; 6th Edition.; W. H. Freeman and Company: New York, 2003.
(19) Dunford, A. J.; Girvan, H. M.; Scrutton, N. S.; Munro, A. W. Probing the Molecular Determinants of Coenzyme Selectivity in the P450 BM3 FAD/NADPH Domain. *Biochim. Biophys. Acta* **2009**, *1794*, 1181–1189.